

CORNERED BUT ALIVE:

GeV-SCALE DARK MATTER FROM DARK PHOTONS

Based on *JHEP* 04 (2026) 083

David Alonso-González (he/him) with D. Cerdéño, P. Foldenauer & J. M. No

PASCOS 2026 (June 23rd, Sheffield)



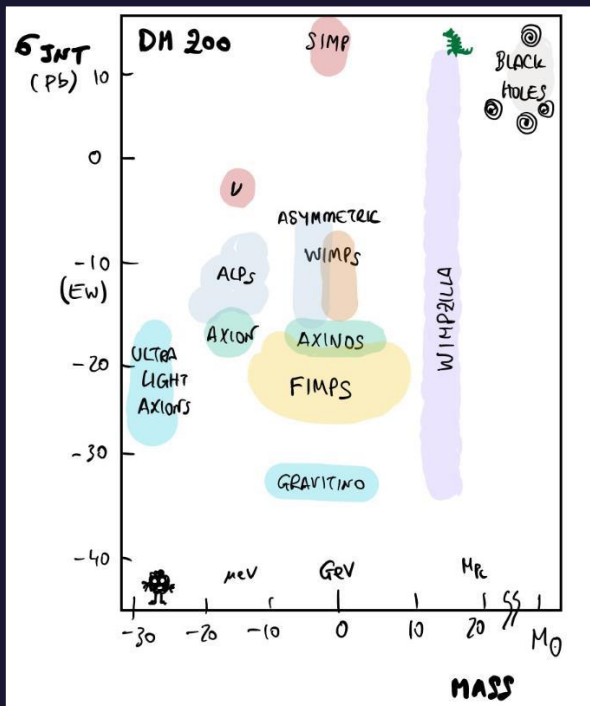
Instituto de
Física
Teórica
UAM-CSIC



Universidad Autónoma
de Madrid

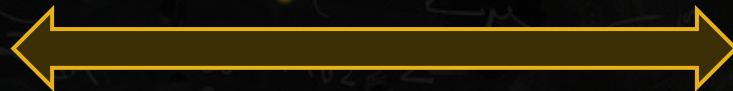


DARK MATTER



Author: David Cerdano

We need a portal to connect them!



DARK PHOTONS

(Vector Portal)

ORDINARY MATTER

Standard Model of Elementary Particles

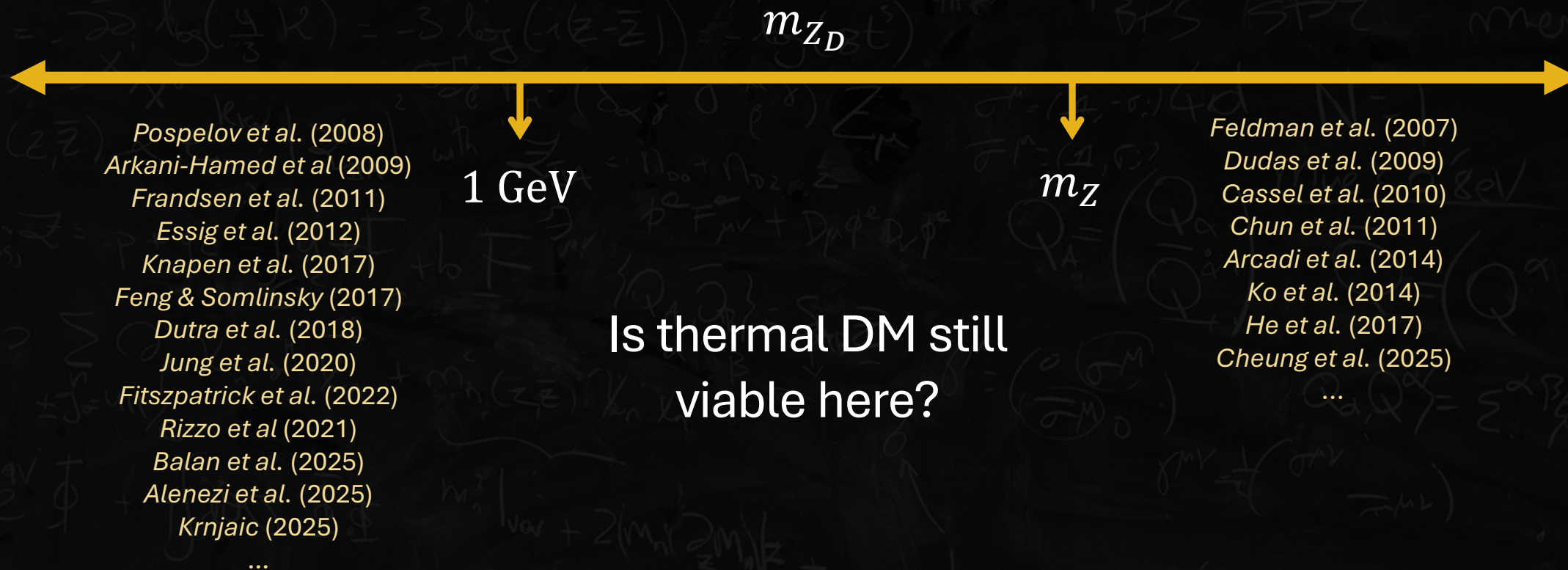
| | three generations of matter (fermions) | | | interactions / force carriers (bosons) | |
|----------------|---|---------------------------------------|--------------------------------------|--|---------------------------|
| | I | II | III | | |
| mass | ≈2.16 MeV/c ² | ≈1.273 GeV/c ² | ≈172.57 GeV/c ² | 0 | ≈125.2 GeV/c ² |
| charge | 2/3 | 2/3 | 2/3 | 0 | 0 |
| spin | 1/2 | 1/2 | 1/2 | 1 | 0 |
| QUARKS | u up | c charm | t top | g gluon | H higgs |
| | ≈4.7 MeV/c ² | ≈93.5 MeV/c ² | ≈4.183 GeV/c ² | 0 | |
| | -1/3 | -1/3 | -1/3 | 0 | |
| | 1/2 | 1/2 | 1/2 | 1 | |
| | d down | s strange | b bottom | γ photon | |
| | ≈0.511 MeV/c ² | ≈105.66 MeV/c ² | ≈1.77693 GeV/c ² | ≈91.188 GeV/c ² | |
| | -1 | -1 | -1 | 0 | |
| | 1/2 | 1/2 | 1/2 | 1 | |
| LEPTONS | e electron | μ muon | τ tau | Z Z boson | |
| | ≈0.8 eV/c ² | <0.17 MeV/c ² | <18.2 MeV/c ² | ≈80.3692 GeV/c ² | |
| | 0 | 0 | 0 | ±1 | |
| | 1/2 | 1/2 | 1/2 | 1 | |
| | ν_e electron neutrino | ν_μ muon neutrino | ν_τ tau neutrino | W W boson | |
| | | | | | |

SCALAR BOSONS

GAUGE BOSONS VECTOR BOSONS

DARK PHOTONS have been widely explored before...

...but not all of them.



DARK PHOTON $\rightarrow SU(3)_C \times SU(2)_L \times U(1)_Y \times U(1)_X$

$$\mathcal{L} \supset -\frac{1}{4} \begin{pmatrix} \hat{B}_{\mu\nu} & \hat{W}_{\mu\nu}^3 & \hat{X}_{\mu\nu} \end{pmatrix} \begin{pmatrix} 1 & 0 & \epsilon \\ 0 & 1 & 0 \\ \epsilon & 0 & 1 \end{pmatrix} \begin{pmatrix} \hat{B}^{\mu\nu} \\ \hat{W}^{3,\mu\nu} \\ \hat{X}^{\mu\nu} \end{pmatrix} + \quad \text{: kinetic terms}$$

$$-(g' j_\mu^Y \quad g j_\mu^3 \quad \hat{g}_D j_\mu^X) \begin{pmatrix} \hat{B}^\mu \\ \hat{W}^{3,\mu} \\ \hat{X}^\mu \end{pmatrix} + \quad \text{: interaction terms}$$

$$+\frac{1}{2} \begin{pmatrix} \hat{B}_\mu & \hat{W}_\mu^3 & \hat{X}_\mu \end{pmatrix} \frac{v^2}{4} \begin{pmatrix} g'^2 & -g'g & 0 \\ -g'g & g^2 & 0 \\ 0 & 0 & \frac{4\hat{M}_{X_0}^2}{v^2} \end{pmatrix} \begin{pmatrix} \hat{B}^\mu \\ \hat{W}^{3,\mu} \\ \hat{X}^\mu \end{pmatrix} \quad \text{: mass terms}$$

$\hat{B}^\mu, \hat{W}^{3,\mu}$: hypercharge $U(1)_Y$ and neutral $SU(2)_L$ SM gauge bosons

g, g' : SM gauge couplings

j_μ^Y, j_μ^3 : SM fermionic currents

\hat{X}^μ : gauge boson of $U(1)_X$

g_D : $U(1)_X$ gauge coupling

j_μ^X : $U(1)_X$ fermion current

ϵ : kinetic mixing

Bauer, Foldenauer (2022)

Fabbrichesi et al. (2020)

DARK PHOTON

After diagonalizing the mass and kinetic terms through mixing angle α we get the physical fields

$$\begin{pmatrix} \hat{B}^\mu \\ \hat{W}^{3,\mu} \\ \hat{X}^\mu \end{pmatrix} \rightarrow \begin{pmatrix} A^\mu \\ Z^\mu \\ Z_D^\mu \end{pmatrix}$$

- true, massless SM photon
- physical Z boson
- physical **DARK PHOTON**

Interaction terms can be written now in terms of physical particles:

$$\begin{aligned} \mathcal{L} \supset & -A^\mu (e j_\mu^{EM}) + \\ & -Z^\mu [g_Z j_\mu^Z (c_\alpha - s_\alpha \delta) + e j_\mu^{EM} (s_\alpha \delta / t_W) - g_D j_\mu^X s_\alpha] + \\ & -Z_D^\mu [g_Z j_\mu^Z (s_\alpha + c_\alpha \delta) - e j_\mu^{EM} (c_\alpha \delta / t_W) + g_D j_\mu^X c_\alpha] \\ & \delta, s_\alpha \propto \epsilon \qquad c_\alpha \propto 1 + \epsilon^2 \end{aligned}$$

Every interaction between the visible and invisible sectors is **supressed by the kinetic mixing**

In this sector of the model, we have introduced two parameters:

$$(\epsilon, g_D)$$

g_D : $U(1)_X$ gauge coupling

ϵ : kinetic mixing

How does the dark photon get its mass?

DARK SCALAR

DARK SCALAR

Arcadi et al. (2019)
Assamagan (2016)

$$V(H, S) = -\mu^2 H^\dagger H + \lambda (H^\dagger H)^2 - \mu_S^2 S^* S + \lambda_S (S^* S)^2 + \lambda_{HS} S^* S H^\dagger H$$

$$H = \frac{1}{\sqrt{2}} \begin{pmatrix} G^\pm \\ h + v + iG^0 \end{pmatrix} \quad : \text{SM Higgs Doublet} \rightarrow v \text{ breaks } SU(2)_L \times U(1)_Y$$

$$S = \frac{s + w + iG'}{\sqrt{2}} \quad : \text{Dark Scalar Singlet} \rightarrow w \text{ breaks } U(1)_X$$

μ_s : scalar mass parameter

$(\mu_s, \lambda_s, \lambda_{hs})$ λ_s : scalar self-coupling parameter

λ_{hs} : scalar-Higgs coupling parameter

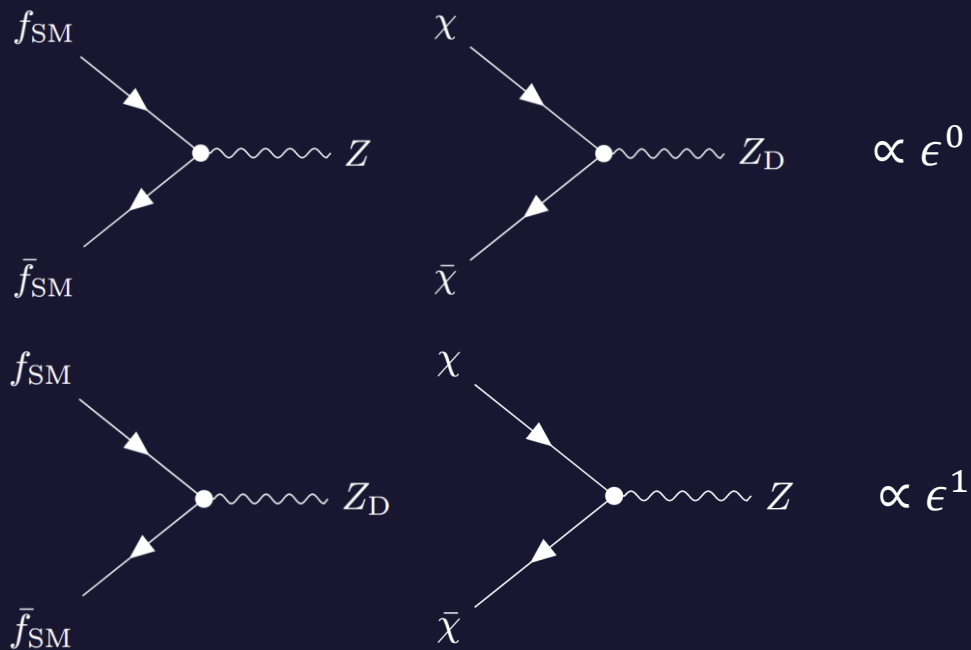
DARK MATTER

(q_χ, m_χ) q_χ : DM charge under $U(1)_X$
 m_χ : DM mass

$$j_\mu^X = q_\chi \bar{\chi} \gamma_\mu \chi$$

with χ a Dirac Fermion

GAUGE-FERMION INTERACTIONS



DAHM-DM

$(\epsilon, g_D, \mu_S, \lambda_S, \lambda_{hs}, q_X, m_\chi)$

$(m_{Z_D}, m_S, m_\chi, \epsilon, s_\theta, g_D, q_X)$

m_{Z_D} : Dark Photon Mass

m_S : Dark Scalar Mass

m_χ : Dark Matter Mass

ϵ : Kinetic Mixing

s_θ : Scalar Mixing

g_D : Dark Gauge Coupling

q_X : DM vectorial charge

IN THE FOLLOWING...

- χ is lighter than Z_D :

$$m_\chi < m_{Z_D}$$

- Mass regime:

$$1 \text{ GeV} < m_{Z_D} < m_Z$$

- χ can be a fraction of the total DM content:

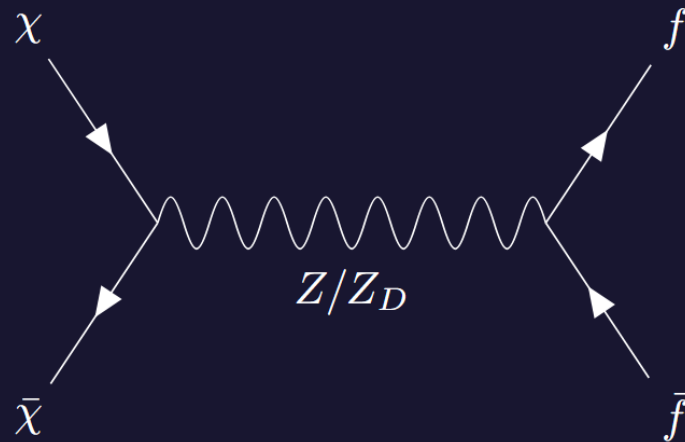
$$\rho_\chi = \tilde{\xi} \rho_{CDM}$$

↑
dilution factor

DM PRODUCTION MECHANISM

FREEZE-OUT

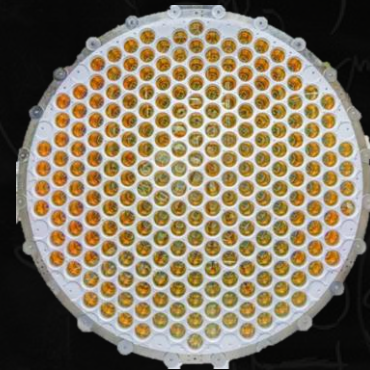
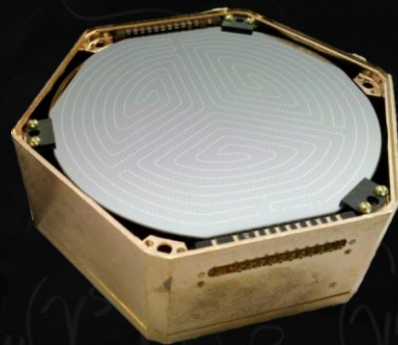
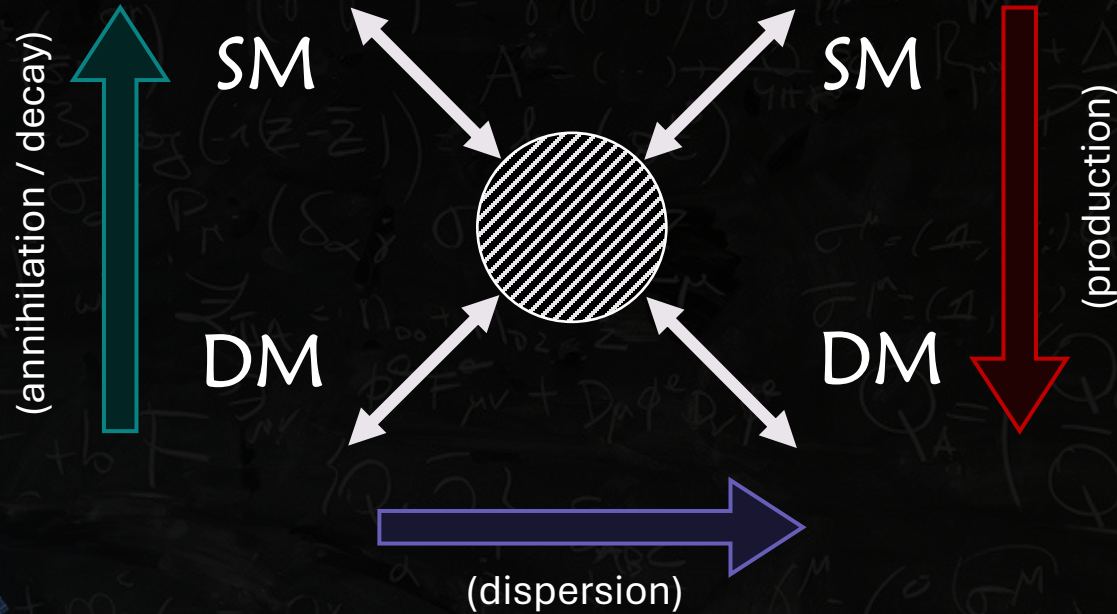
- Dark Matter in thermal equilibrium with plasma at the beginning of the Universe.
- Dark Matter density *freezes-out* when interactions fall below the Hubble rate.
- Weak coupling with SM particles.
- DM relic abundance can be computed solving the Boltzmann equation



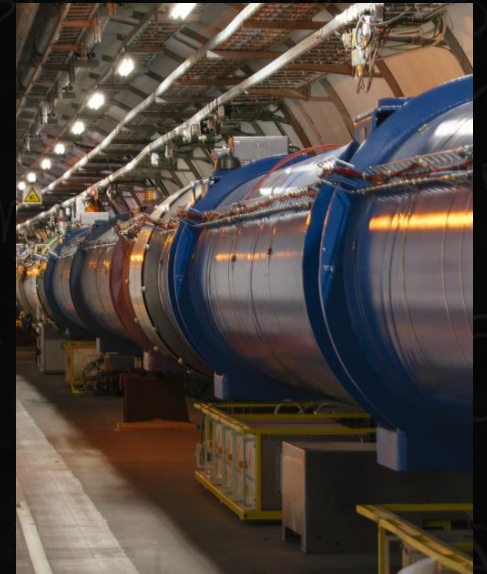
$$\sigma_{ann} \propto \frac{\epsilon^2 \alpha_D \alpha_{EM}}{(s - m_{Z_D}^2)^2 + m_{Z_D}^2 \Gamma_{Z_D}^2}$$

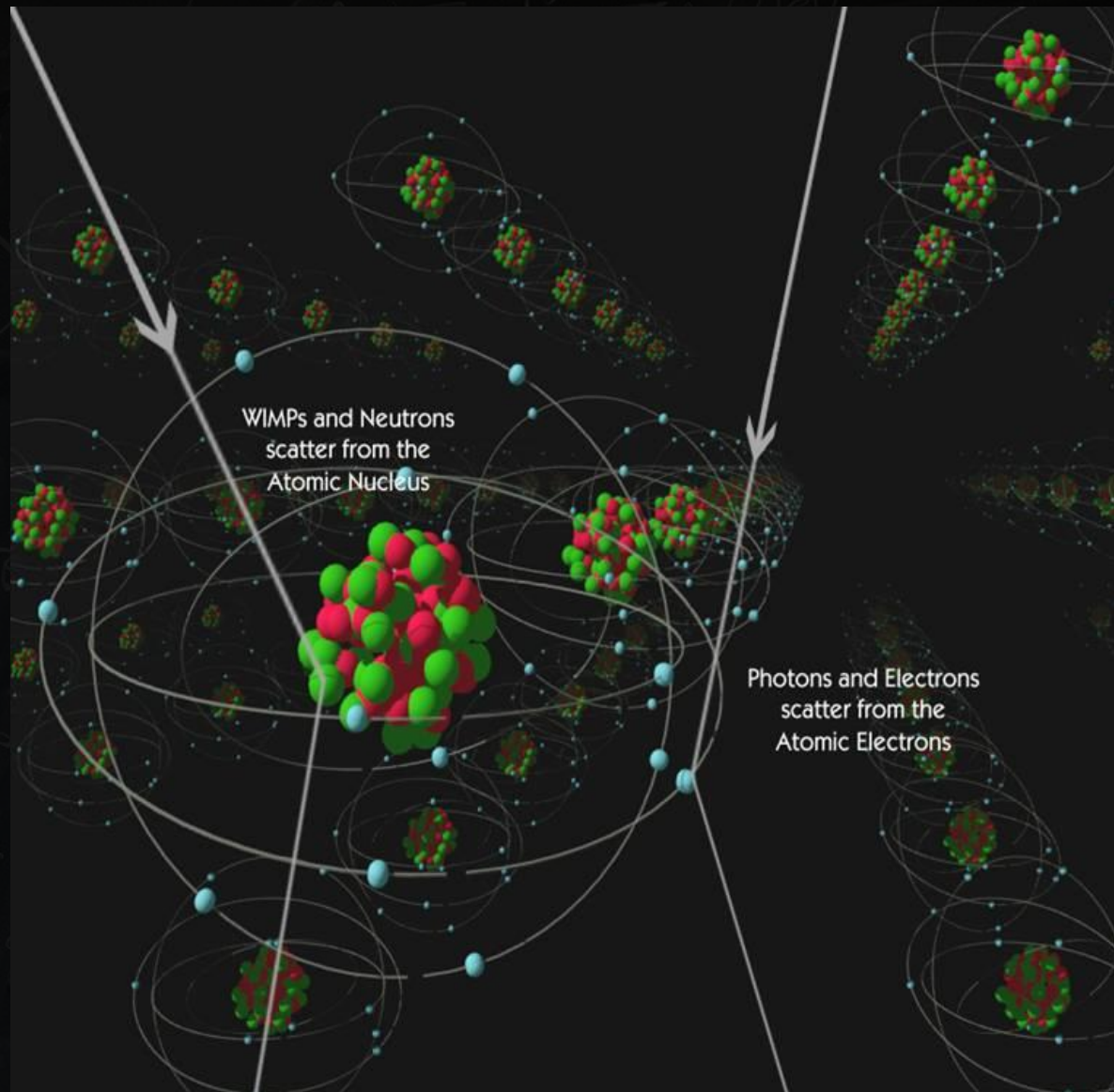
$$\alpha = \frac{e^2}{4\pi} ; \alpha_D = \frac{g_D^2}{4\pi}$$

CORNERING DAHM-DM



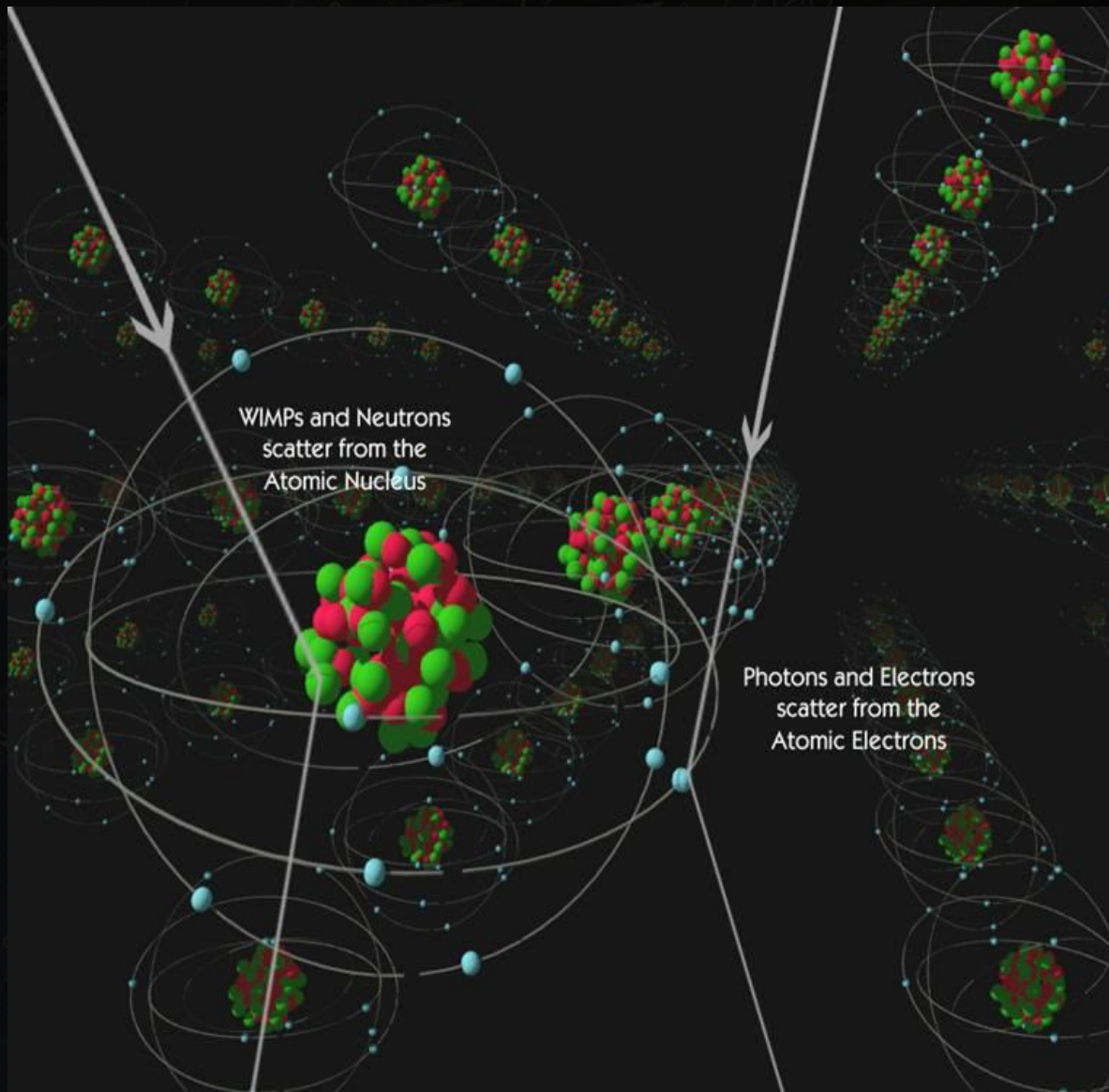
COLLIDERS





DARK MATTER DIRECT DETECTION EXPERIMENTS

University Of California, Berkeley

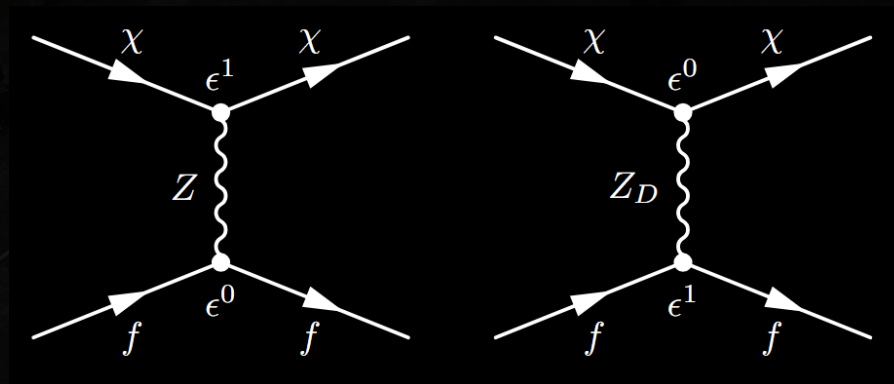


University Of California, Berkeley

Rate of DM-induced nuclear recoils per recoil energy:

$$\frac{dR}{dE_R} = \frac{\xi \rho_0}{m_T m_\chi} \epsilon(E_R) \int dE'_R \text{Gauss}(E'_R, E_R) \int_{v_{\min}} d^3v v f(\vec{v}) \frac{d\sigma_{\chi T}}{dE'_R}$$

DD set constraints on the product $\xi \frac{d\sigma_{\chi T}}{dE'_R}$



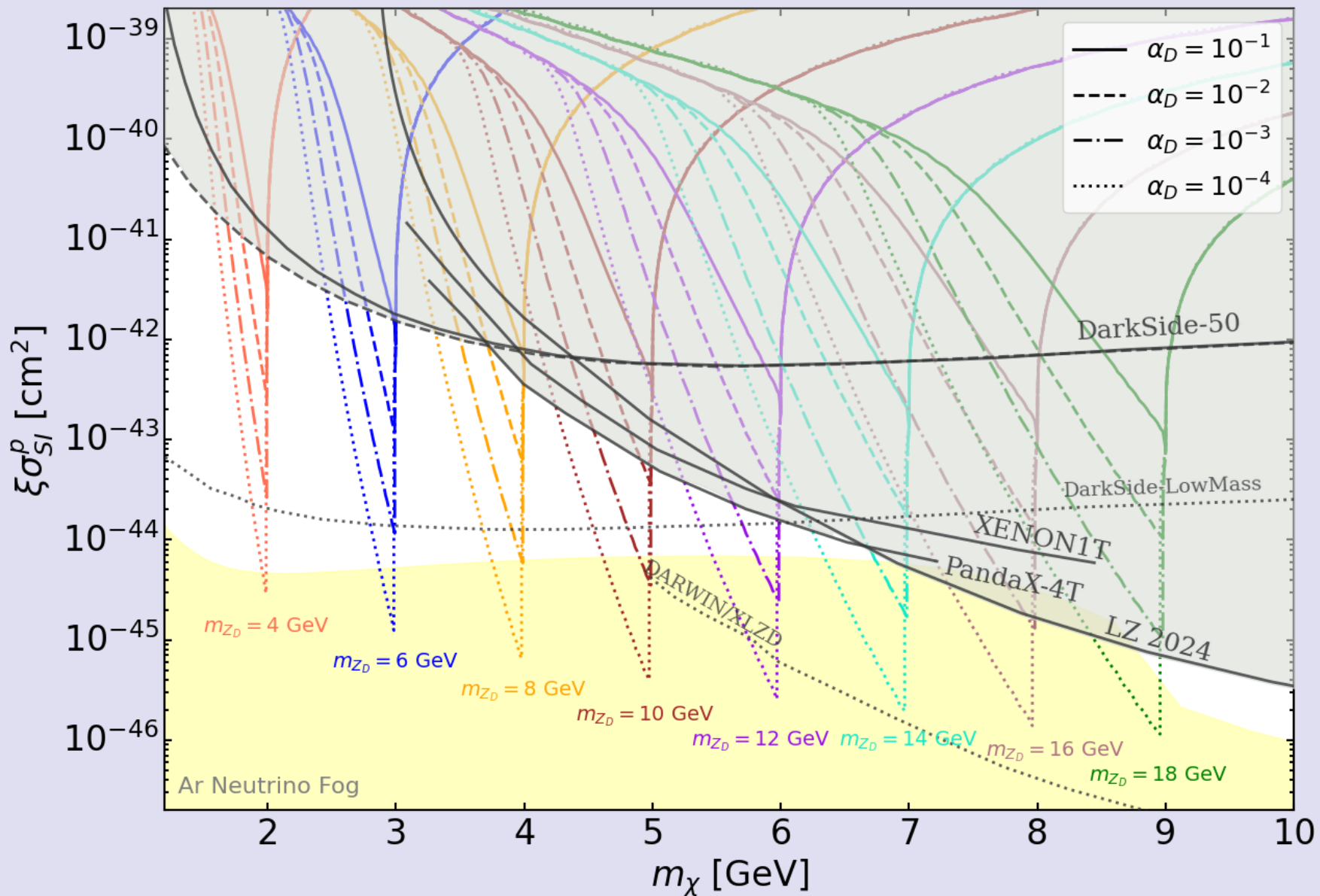
$$\frac{d\sigma_{\chi T}^{SI}}{dE'_R} = \frac{m_T}{2\pi v^2} g_D^2 \epsilon^2 A^2 F^2(E_R) \left| \frac{f_n^{(Z_D)}}{m_{Z_D}^2} + \frac{f_n^{(Z)} s_W}{m_Z^2 - m_{Z_D}^2} \right|^2$$

$$f_n^{(X)} = \frac{1}{A} (Z f_{p,X} + (A - Z) f_{n,X})$$

$$f_{p,X} = 2g_{u,X} + g_{d,X}$$

$$f_{n,X} = g_{u,X} + 2g_{d,X} \rightarrow 0$$

DIRECT DETECTION BOUNDS



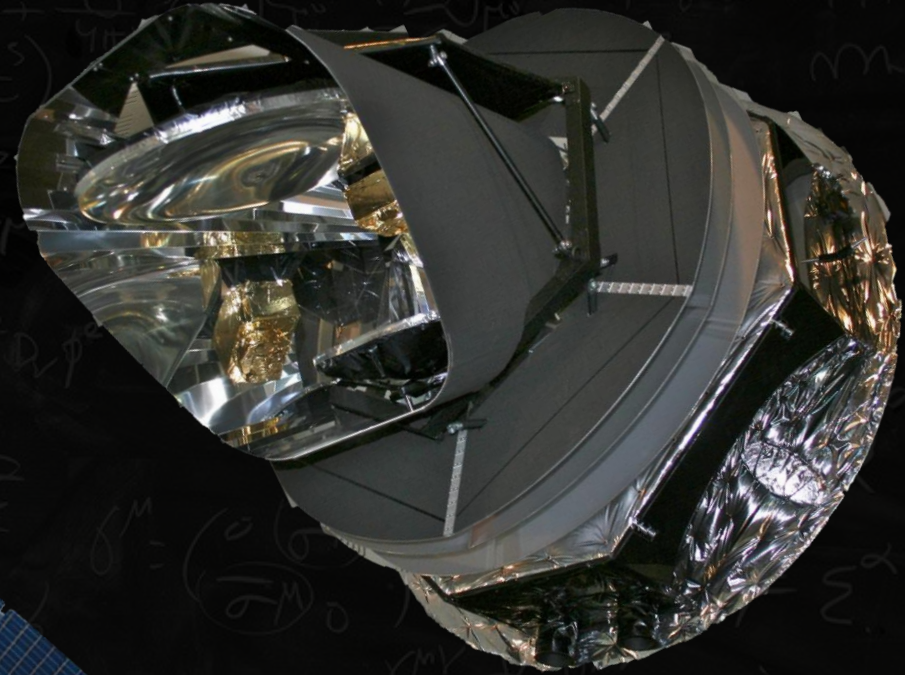
$$\sigma_{SI}^p \propto \epsilon^2$$

$$\xi \propto 1/\langle\sigma v\rangle \propto \epsilon^{-2}$$

DD bounds are independent of the value of ϵ

- XENON collaboration (2021)
- DarkSide-50 collaboration (2023)
- PandaX-4T collaboration (2021)
- LZ collaboration (2025)
- Global Argon Dark Matter collaboration (2023)
- DARWIN collaboration (2016)
- XLZD collaboration (2024)
- O'Hare (2021)

Fermi-Large Area Telescope (LAT)



Planck Satellite

DARK MATTER INDIRECT DETECTION

GAMMA RAYS FROM DWARF SPHEROIDAL GALAXIES (dSphs)

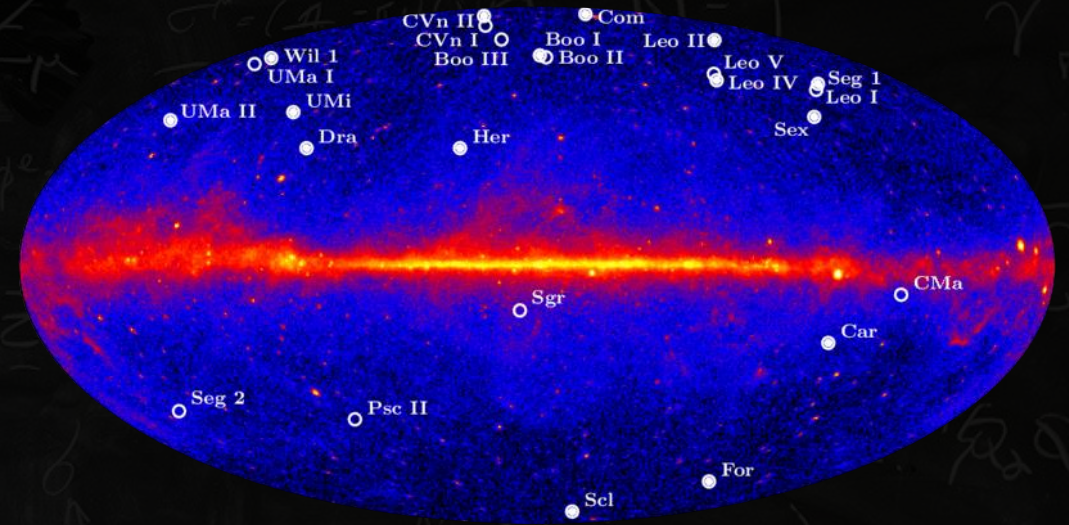
dSphs are some of the most DM-rich environments in the universe, so we can set DM constraints from the observation of gamma rays from them.

Gamma Ray flux per solid angle:

$$\frac{d\Phi}{dE}(\Delta\Omega) = \frac{J}{4\pi} \sum_f \frac{\langle\sigma v\rangle_f}{2m_\chi^2} \frac{dN_\gamma^f}{dE}$$

$$J = \int_{\Delta\Omega} d\Omega \int dl \underbrace{\rho_\chi^2(r)}$$

gamma-ray flux will be re-scaled by $\propto \xi^2$



Fermi-LAT collaboration (2014)

GAMMA RAYS FROM DWARF SPHEROIDAL GALAXIES (dSphs)

dSphs are some of the most DM-rich environments in the universe, so we can set DM constraints from the observation of gamma rays from them.

Gamma Ray flux per solid angle:

$$\frac{d\Phi}{dE}(\Delta\Omega) = \frac{J}{4\pi} \sum_f \frac{\langle\sigma v\rangle_f}{2m_\chi^2} \frac{dN_\gamma^f}{dE}$$

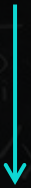
$$J = \int_{\Delta\Omega} d\Omega \int dl \underbrace{\rho_\chi^2(r)}_{\text{gamma-ray flux will be re-scaled by } \propto \xi^2}$$

gamma-ray flux will be re-scaled by $\propto \xi^2$

McDaniel, Ajello, Karwin, Di Mauro, Drlica-Wagner & Sánchez-Conde (2024)

| (1) Name | (2) R.A. (J2000) [deg] | (3) Decl. (J2000) [deg] | (4) Distance [kpc] | (5) $r_{1/2}$ [pc] | (6) M_V [mag] | (7) $\sigma_{l.o.s.}$ [km s ⁻¹] | (8) $\log_{10} J \pm \sigma_J$ [log ₁₀ GeV ² cm ⁻⁵] |
|----------------------------------|------------------------------|-------------------------------|--------------------------|--------------------------|-----------------------|---|---|
| dSphs with Measured J -factors | | | | | | | |
| Aquarius II | 338.48 | -9.33 | 108.0 | 125 | -4.4 | 4.7 ^a | 17.80 ± 0.55 ^a |
| Boötes II | 209.51 | 12.86 | 42.0 | 39 | -2.94 | 2.9 ^a | 18.30 ± 0.95 ^a |
| Canes Venatici I | 202.01 | 33.55 | 218.0 | 338 | -8.8 | 7.6 | 17.42 ± 0.16 |
| Canes Venatici II | 194.29 | 34.32 | 160.0 | 55 | -5.17 | 4.7 | 17.82 ± 0.47 |
| Carina | 100.41 | -50.96 | 105.0 | 248 | -9.43 | 6.4 | 17.83 ± 0.10 |
| Carina II | 114.11 | -58.0 | 36.0 | 77 | -4.5 | 3.4 | 18.25 ± 0.55 |
| Coma Berenices | 186.75 | 23.91 | 44.0 | 57 | -4.38 | 4.7 | 19.00 ± 0.35 |
| Draco | 260.07 | 57.92 | 76.0 | 180 | -8.71 | 9.1 | 18.83 ± 0.12 |
| Draco II | 238.17 | 64.58 | 22.0 | 17 | -0.8 | 3.4 | 18.93 ± 1.54 |
| Eridanus II | 56.09 | -43.53 | 380.0 | 158 | -7.21 | 7.1 | 16.60 ± 0.90 |
| Fornax | 39.96 | -34.5 | 147.0 | 707 | -13.46 | 10.6 | 18.09 ± 0.10 |
| Grus I | 344.18 | -50.18 | 120.0 | 21 | -3.47 | 4.5 | 16.50 ± 0.80 |
| Hercules | 247.77 | 12.79 | 132.0 | 120 | -5.83 | 3.9 | 17.37 ± 0.53 |
| Horologium I | 43.88 | -54.12 | 79.0 | 31 | -3.55 | 5.9 | 19.00 ± 0.81 |
| Hydrus I | 37.39 | -79.31 | 28.0 | 53 | -4.71 | 2.7 ^b | 18.33 ± 0.36 ^b |
| Leo I | 152.11 | 12.31 | 254.0 | 226 | -11.78 | 9.0 | 17.64 ± 0.13 |
| Leo II | 168.36 | 22.15 | 233.0 | 165 | -9.74 | 7.4 | 17.76 ± 0.20 |
| Leo IV | 173.24 | -0.55 | 154.0 | 104 | -4.99 | 3.4 | 16.40 ± 1.08 |
| Leo V | 172.79 | 2.22 | 178.0 | 39 | -4.4 | 4.9 | 17.65 ± 0.97 |
| Pegasus III | 336.1 | 5.41 | 215.0 | 42 | -3.4 | 7.9 | 18.30 ± 0.93 |
| Pisces II | 344.63 | 5.95 | 182.0 | 48 | -4.22 | 4.8 | 17.30 ± 1.04 |
| Reticulum II | 53.92 | -54.05 | 30.0 | 31 | -3.88 | 3.4 | 18.90 ± 0.38 |
| Sagittarius II | 298.16 | -22.07 | 69.0 | 32 | -5.2 | 2.7 ^c | 17.35 ± 1.36 ^d |
| Segue 1 | 151.75 | 16.08 | 23.0 | 20 | -1.3 | 3.1 | 19.12 ± 0.53 |
| Sextans | 153.26 | -1.61 | 86.0 | 345 | -8.72 | 7.1 | 17.73 ± 0.12 |
| Tucana II | 342.98 | -58.57 | 58.0 | 165 | -3.8 | 7.3 | 18.97 ± 0.54 |
| Tucana IV | 0.73 | -60.85 | 48.0 | 128 | -3.5 | 4.3 ^e | 18.40 ± 0.55 ^e |
| Ursa Major I | 158.77 | 51.95 | 97.0 | 151 | -5.12 | 7.3 | 18.26 ± 0.28 |
| Ursa Major II | 132.87 | 63.13 | 32.0 | 85 | -4.25 | 7.2 | 19.44 ± 0.40 |
| Ursa Minor | 227.24 | 67.22 | 76.0 | 272 | -9.03 | 9.3 | 18.75 ± 0.12 |

$\xi^2 \langle \sigma v \rangle$ increases
as ϵ decreases

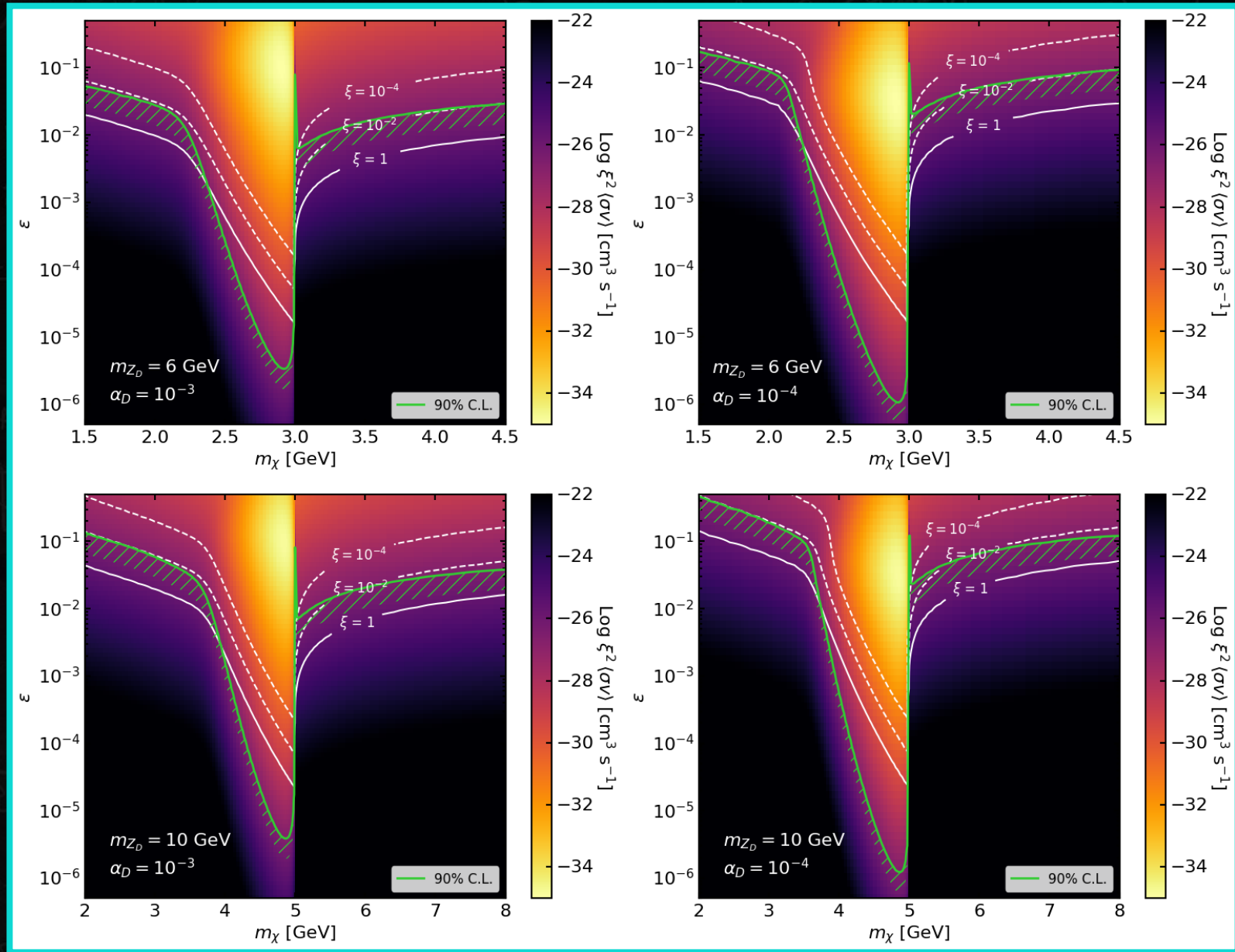


Gamma ray flux
increases as ϵ
decreases



We obtain a
lower bound on ϵ
(and on $\xi^2 \langle \sigma v \rangle$)

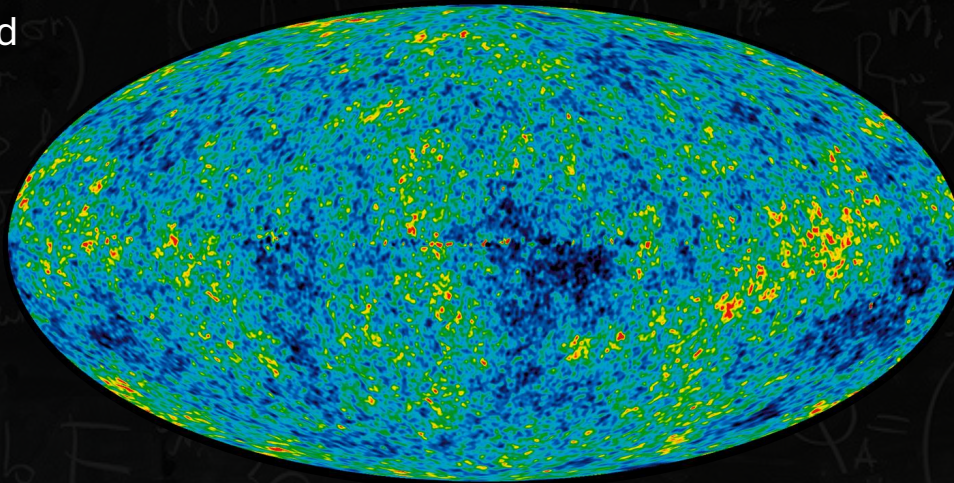
McDaniel, Ajello, Karwin, Di Mauro,
Drlica-Wagner & Sánchez-Conde (2024)



GAMMA RAYS BOUNDS

CMB IONISATION CONSTRAINTS

Since DM can annihilate into charged SM particles, it can reintroduce a certain amount of ionization during and after recombination



This amount of extra ionization can be constrained with the CMB, since it would distort the theoretically clean CMB polarization spectrum

Rate of released energy into the primordial bath of particles from DM annihilations:

$$\frac{d^2 E}{dV dt} = \rho_\chi^2 (1+z)^6 P_{ann}(z)$$

energy rate will be re-scaled by $\propto \xi^2$

$$\text{with } P_{ann}(z) = \sum_i f_i(z) \frac{\langle \sigma v \rangle_i}{m_\chi}$$

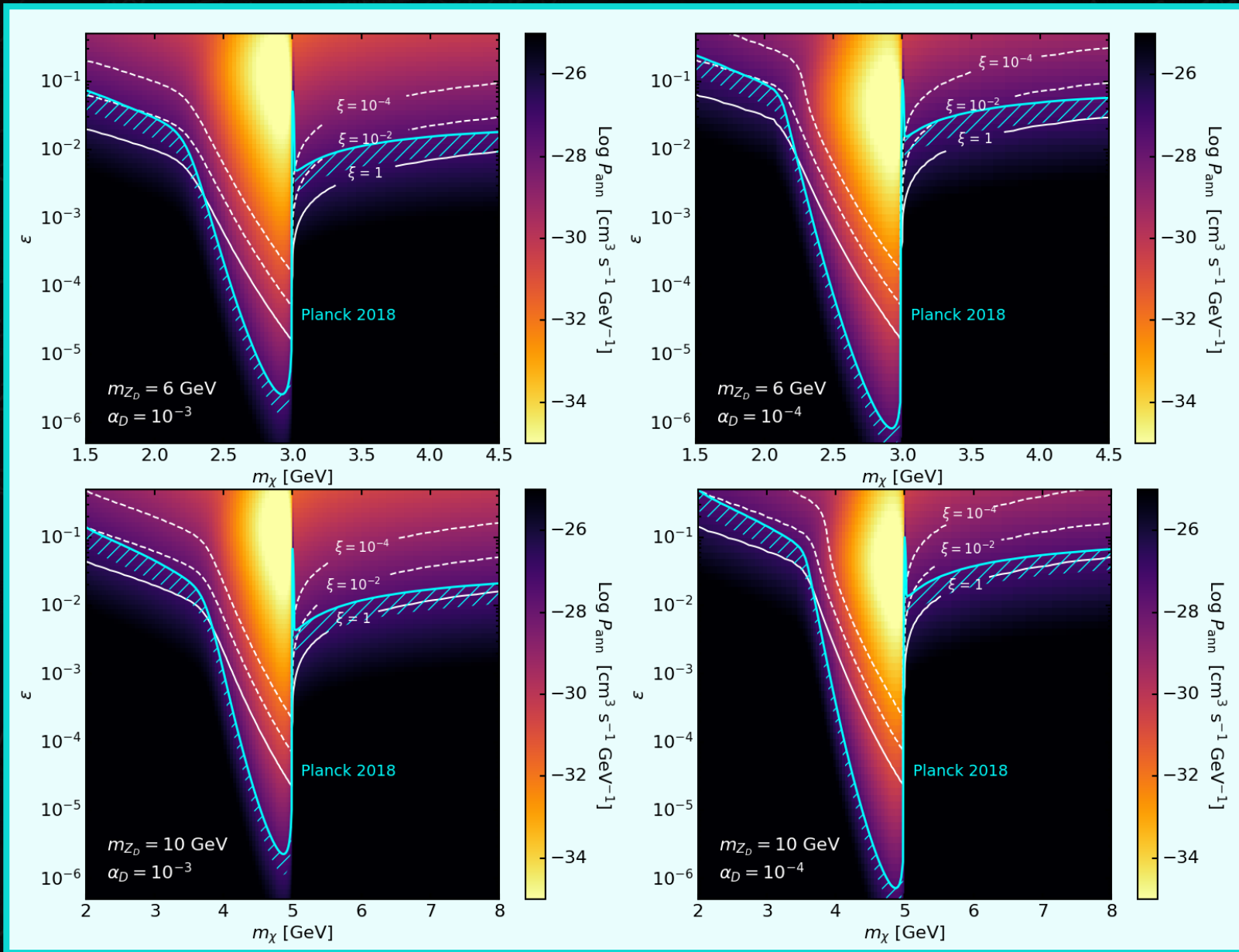
...constrained by the Planck mission from CMB anisotropies measurement

$$P_{ann} < 3.5 \times 10^{-28} \text{ cm}^2 \text{ s}^{-1} \text{ GeV}^{-1}$$

For each annihilation channel i:

- $\langle \sigma v \rangle_i$ thermal average annihilation cross-section
- $f_i(z)$ redshift-dependent ionization efficiency factor

CMB BOUNDS



$P_{ann} \propto \xi^2$ increases
as ϵ decreases

We obtain a
lower bound on ϵ

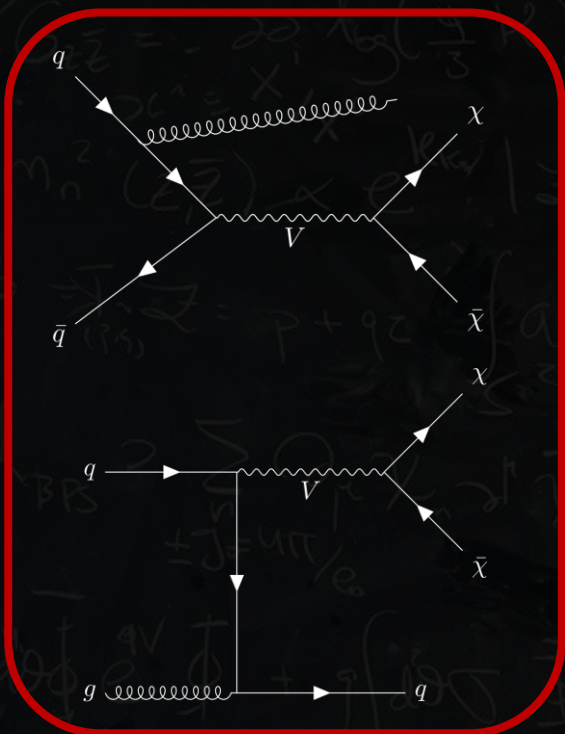
Planck collaboration (2020)

COLLIDER SEARCHES

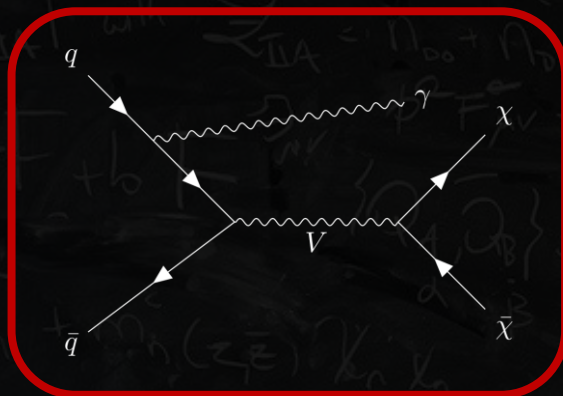


INVISIBLE SEARCHES

If $m_{Z_D} > 2m_\chi$, the decay channel $Z_D \rightarrow \bar{\chi}\chi$ is kinematically open and dominates the decay width



MONO-JET SEARCHES IN LHC



MONO-PHOTON SEARCHES IN LEP AND BaBar

VISIBLE SEARCHES

Given the strong sensitivity of di-lepton searches, they can still be relevant, in particular when $\alpha_D \ll \alpha_{EM}\epsilon^2$

$$\Gamma_{Z_D} = \Gamma_{Z_D \rightarrow SM} + \Gamma_{Z_D \rightarrow \bar{\chi}\chi}$$

$$\epsilon < \epsilon_{90}^{ll} \times \sqrt{\frac{\Gamma_{Z_D \rightarrow SM} + \Gamma_{Z_D \rightarrow \bar{\chi}\chi}}{\Gamma_{Z_D \rightarrow SM}}}$$

90% C.L. di-lepton limit for $\Gamma_{Z_D \rightarrow \bar{\chi}\chi} = 0$

- BaBar collaboration (2017)*
- LHCb collaboration (2020)*
- CMS collaboration (2020)*
- CMS collaboration (2023)*

EW PRECISION OBSERVABLES

Our model introduces modifications on the couplings of the Z-boson with the SM fermion content that depend on its mixing with the dark photon



Electroweak precision observables yield an indirect constraint on the kinetic mixing parameter ϵ

Parametrization of the neutral current interactions of physical Z-boson with SM fermions:

$$\mathcal{L}_{NC} = \frac{-e}{s_W c_W} \left(1 + \frac{\alpha_{EM} T}{2} \right) \bar{f}_i \gamma^\mu \left[T_{3i} P_L - Q_i \left(s_W^2 + \frac{\alpha_{EM} S}{4(c_W^2 - s_W^2)} - \frac{c_W^2 s_W^2 \alpha_{EM} T}{c_W^2 - s_W^2} \right) \right] f_i Z_\mu$$

In DAHM-DM:

$$\mathcal{L}_{NC} = \frac{-e}{s_W c_W} c_\alpha \bar{f}_i \gamma^\mu \left[T_{3i} P_L \left(1 - \frac{s_\alpha}{c_\alpha} \delta \right) - Q_i \left(s_W^2 - \frac{s_\alpha}{c_\alpha} \delta \right) \right] f_i Z_\mu$$

By comparison:

$$S(\epsilon, m_{Z_D})$$

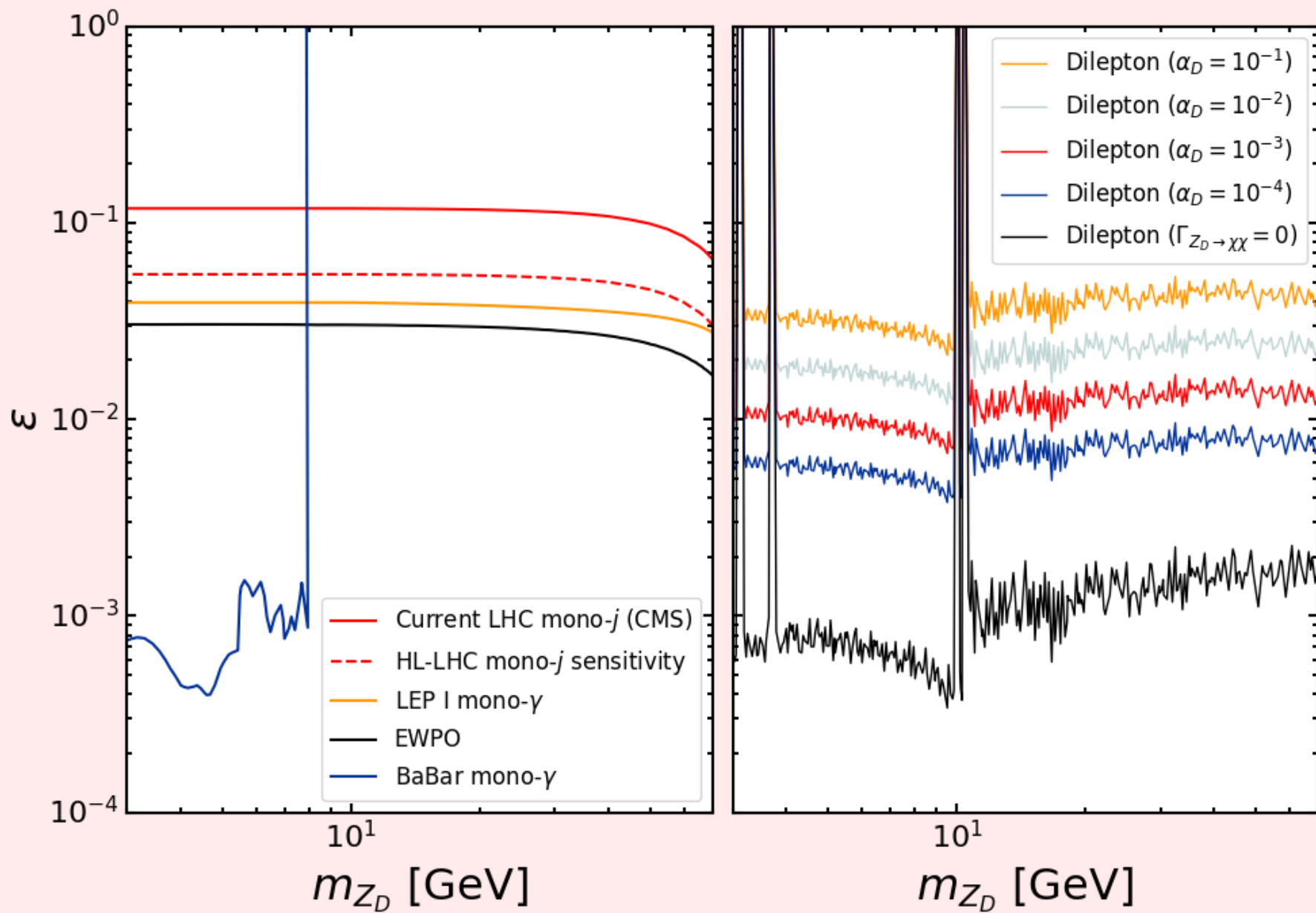
$$T(\epsilon, m_{Z_D})$$

OBLIQUE PARAMETERS

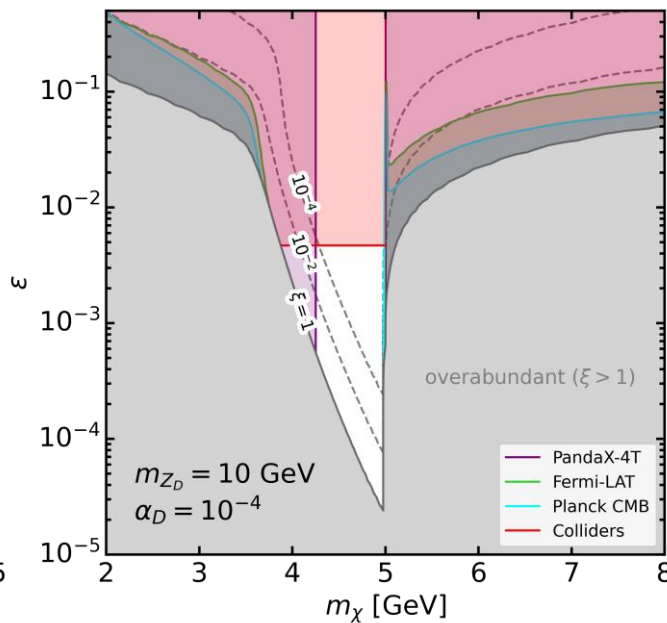
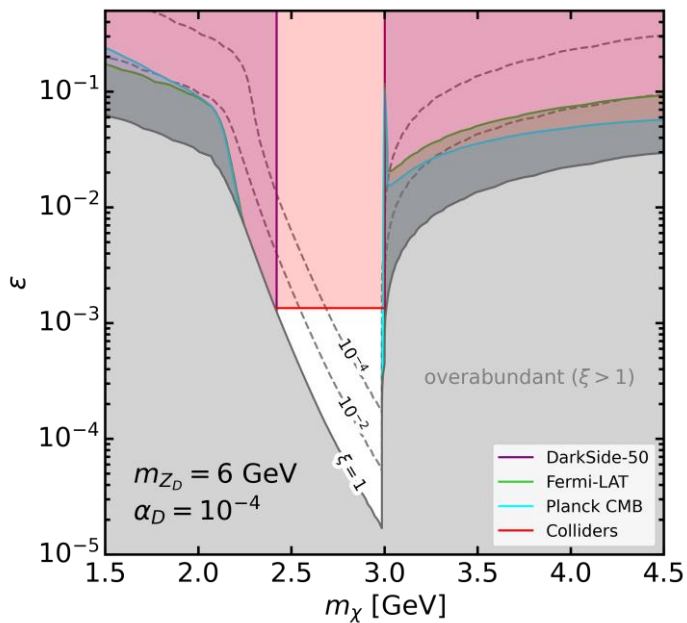
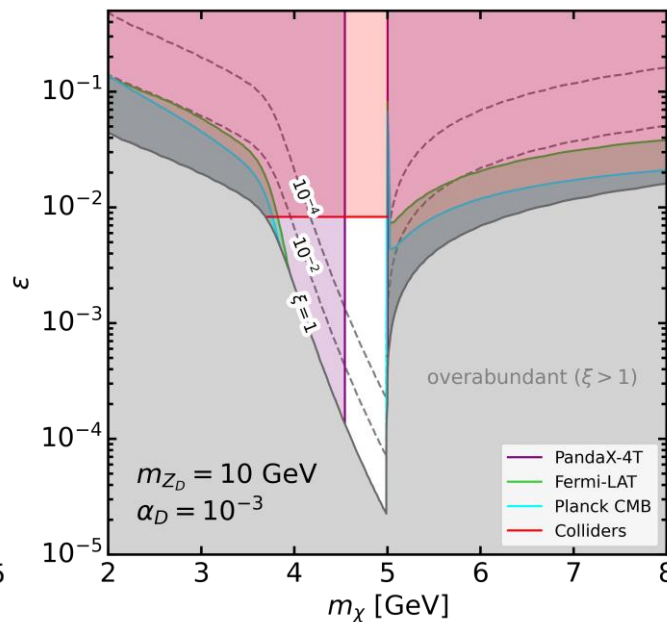
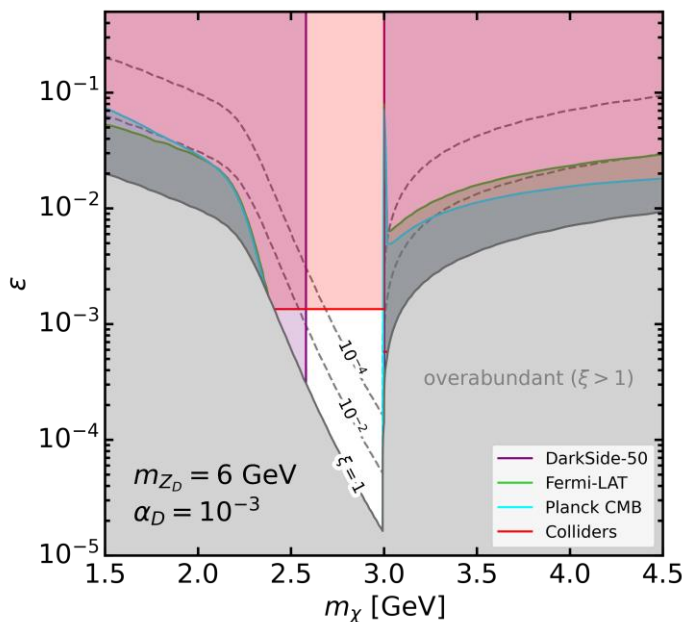
$$S = -0.05 \pm 0.07$$

$$T = 0.00 \pm 0.06$$

Particle Data Group (2024)



DELPHI collaboration (2009)
 BaBar collaboration (2017)
 LHCb collaboration (2020)
 CMS collaboration (2020)
 CMS collaboration (2023)



CONCLUSIONS

- DD, ID and colliders probe complementary regions of the parameter space.
- Scenarios with large α_D are ruled out by DD, even in the resonance regime.
- ID constraints are relevant for $\xi \rightarrow 1$ and away from the resonant region.
- Next generation DD experiments will be able to probe most of the remaining allowed resonant DM scenarios.
- Current and future collider searches can probe complementary regions with sizeable kinetic mixing.

thanks for your attention!



BACKUP SLIDES

THERMAL CROSS SECTION

$$\frac{d\sigma}{dt} = \frac{1}{64 \pi s} \frac{1}{|\vec{p}_1|_{\text{CM}}^2} \overline{|\mathcal{M}|^2} = \frac{1}{16 \pi s (s - 4m_\chi^2)} \overline{|\mathcal{M}|^2},$$

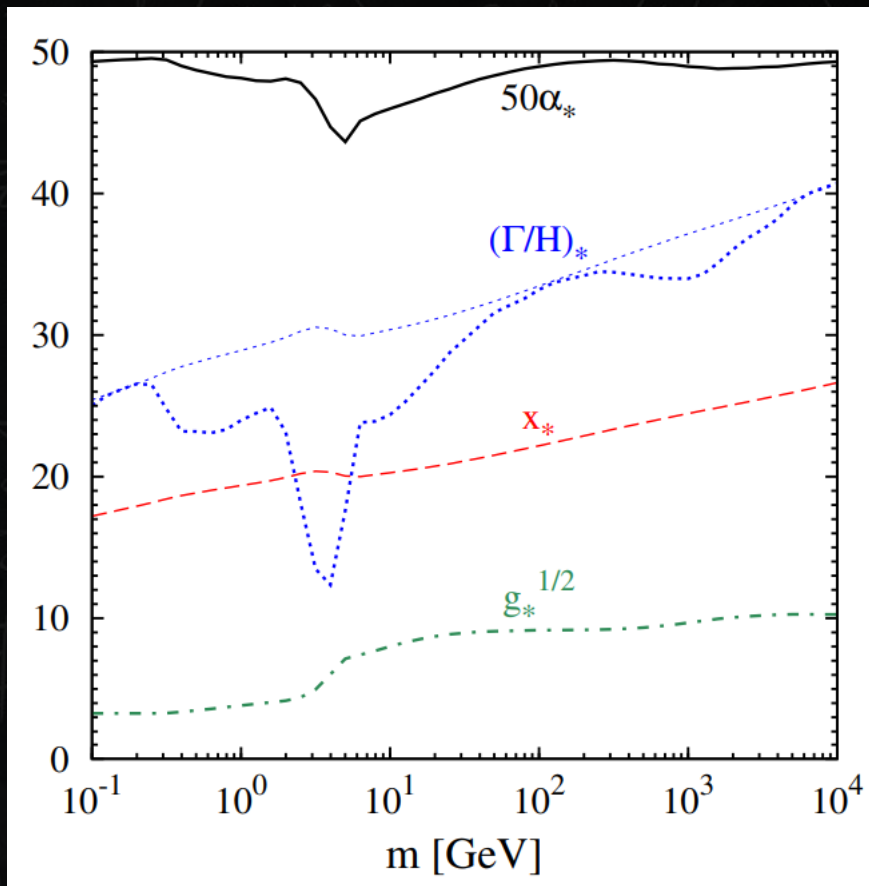
$$t = \left[\frac{m_1^2 - m_2^2 - m_3^2 + m_4^2}{s\sqrt{s}} \right]^2 - \left(|\vec{p}_1|_{\text{CM}}^2 - 2|\vec{p}_1|_{\text{CM}} |\vec{p}_3|_{\text{CM}} \cos \theta + |\vec{p}_3|_{\text{CM}}^2 \right)$$

$$\langle \sigma v \rangle_{\text{CM}} = \frac{x}{2 [K_1^2(x) + K_2^2(x)]} \int_2^\infty dz \sigma(z^2 m_\chi^2) (z^2 - 4) z^2 K_1(zx), \quad (\text{B.5})$$

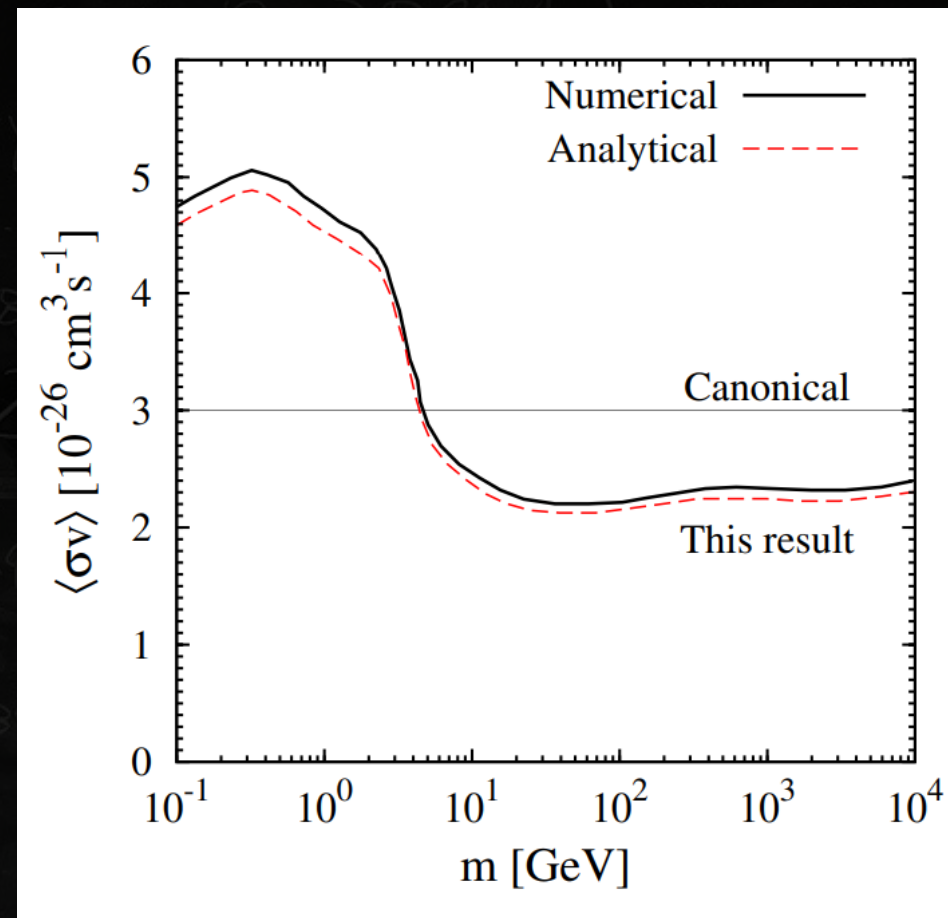
where $x = m_\chi/T$, $z = \sqrt{s}/m_\chi$ and $K_n(x)$ denote the modified Bessel functions of the second kind.

$$\Omega = \frac{m Y_f s_0}{\rho_{crit}}$$

$$= \frac{8\pi G}{3H_0^2} \left(\frac{m H_* s_0}{\langle \sigma v \rangle s_*} \right) \left(\frac{(\Gamma/H)_*}{1 + \alpha_* (\Gamma/H)_*} \right)$$



Steigman et al. [1204.3622]



$$\frac{dY}{dx} = \frac{s \langle \sigma v \rangle}{Hx} \left[1 + \frac{1}{3} \frac{d(\ln g_s)}{d(\ln T)} \right] (Y_{eq}^2 - Y^2)$$

Dark matter Relic Abundance beyond Kinetic Equilibrium

Tobias Binder^{1,a}, Torsten Bringmann^{2,b}, Michael Gustafsson^{3,c},
Andrzej Hryczuk^{4,d}

¹Kavli IPMU (WPI), UTIAS, The University of Tokyo, Kashiwa, Chiba 277-8583, Japan

²Department of Physics, University of Oslo, Box 1048 Blindern, NO-0316 Oslo, Norway

³Institute for Theoretical Physics, Georg-August University Göttingen, Friedrich-Hund-Platz 1, D-37077 Göttingen, Germany

⁴National Centre for Nuclear Research, Pasteura 7, 02-093 Warsaw, Poland

$$E(\partial_t - Hp\partial_p)f_\chi = C_{\text{ann}}[f_\chi] + C_{\text{el}}[f_\chi], \quad (1)$$

where

$$C_{\text{ann}} = \frac{1}{2g_\chi} \int \frac{d^3\tilde{p}}{(2\pi)^3 2\tilde{E}} \int \frac{d^3k}{(2\pi)^3 2\omega} \int \frac{d^3\tilde{k}}{(2\pi)^3 2\tilde{\omega}} \quad (2)$$

$$\times (2\pi)^4 \delta^{(4)}(\tilde{p} + p - \tilde{k} - k)$$

$$\times \left[|\mathcal{M}|_{\tilde{\chi}\chi \leftarrow \tilde{f}f}^2 g(\omega)g(\tilde{\omega}) - |\mathcal{M}|_{\tilde{\chi}\chi \rightarrow \tilde{f}f}^2 f_\chi(E)f_\chi(\tilde{E}) \right]$$

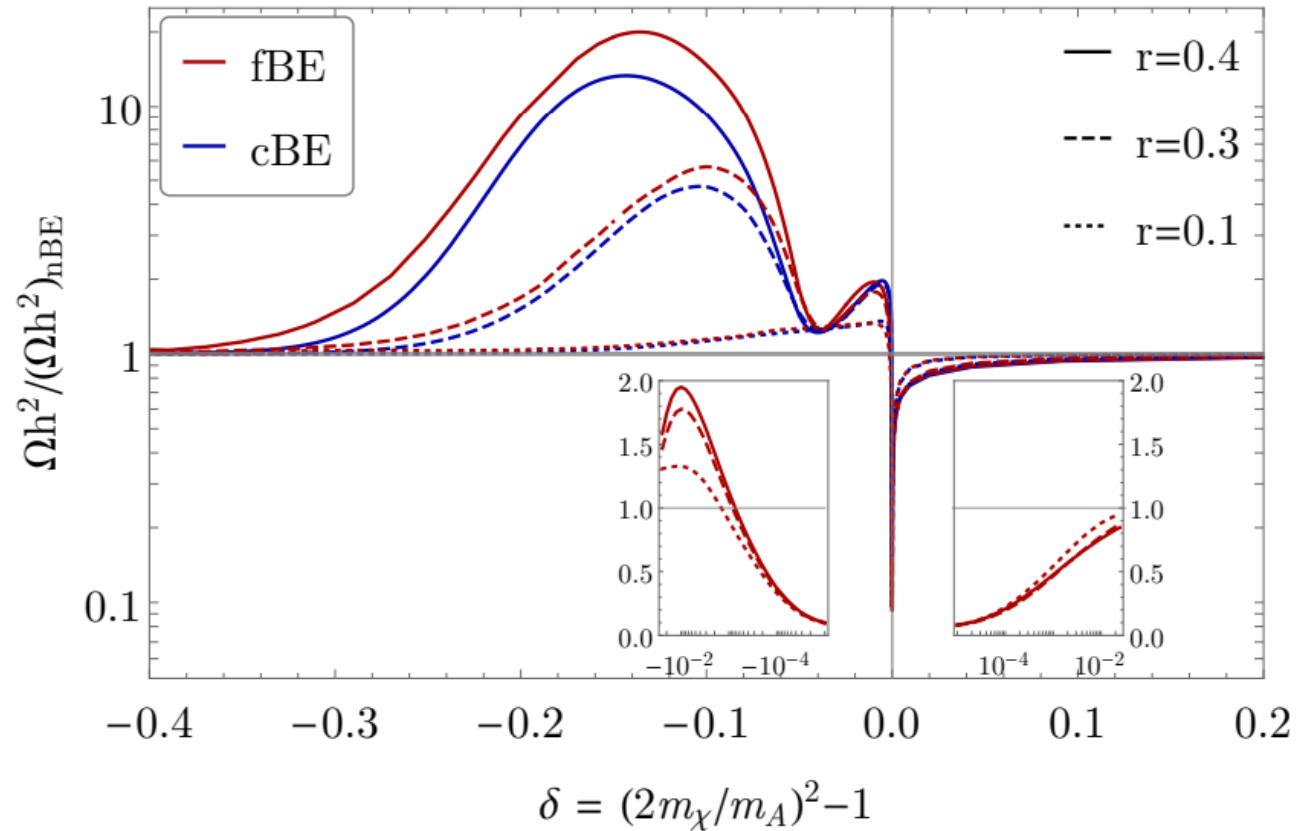
describes the effect of two-body annihilations, and the collision term for elastic scattering processes is given by

$$C_{\text{el}} = \frac{1}{2g_\chi} \int \frac{d^3k}{(2\pi)^3 2\omega} \int \frac{d^3\tilde{k}}{(2\pi)^3 2\tilde{\omega}} \int \frac{d^3\tilde{p}}{(2\pi)^3 2\tilde{E}} \quad (3)$$

$$\times (2\pi)^4 \delta^{(4)}(\tilde{p} + \tilde{k} - p - k) |\mathcal{M}|_{\chi f \leftrightarrow \chi f}^2$$

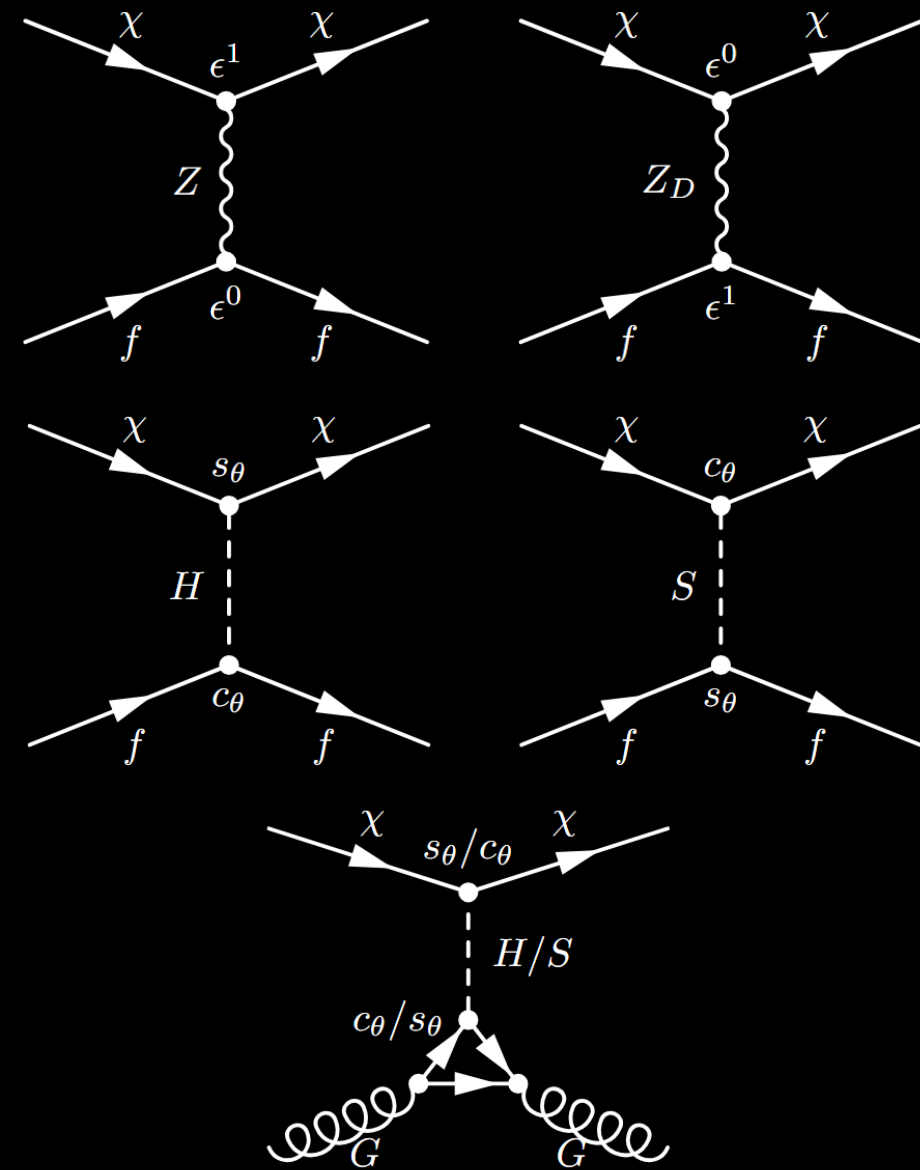
$$\times \left[(1 \mp g^\pm(\omega)) g^\pm(\tilde{\omega}) f_\chi(\tilde{E}) - (\omega \leftrightarrow \tilde{\omega}, E \leftrightarrow \tilde{E}) \right].$$

$$\dot{n} + 3Hn = -\langle\sigma v\rangle_T [n^2 - n_{\text{eq}}^2(T)],$$



NON-RELATIVISTIC EFFECTIVE FIELD THEORY

$$\mathcal{L}_{NREFT} = \sum_{i,N} c_i^N(q^2) \mathcal{O}_i^N$$



NON-RELATIVISTIC EFFECTIVE FIELD THEORY

$$\mathcal{L}_{NREFT} = \sum_{i,N} c_i^N(q^2) \mathcal{O}_i^N$$

Bishara et al. [1707.06998]

$$\mathcal{O}_1^N = \mathbb{1}_X \mathbb{1}_N$$

$$\mathcal{O}_2^N = (v_\perp)^2 \mathbb{1}_X \mathbb{1}_N$$

$$\mathcal{O}_3^N = \mathbb{1}_X \vec{S}_N \cdot \left(\vec{v}_\perp \times \frac{i\vec{q}}{m_N} \right)$$

$$\mathcal{O}_4^N = \vec{S}_X \cdot \vec{S}_N$$

$$\mathcal{O}_5^N = \vec{S}_X \cdot \left(\vec{v}_\perp \times \frac{i\vec{q}}{m_N} \right)$$

$$\mathcal{O}_6^N = \left(\vec{S}_X \cdot \frac{\vec{q}}{m_N} \right) \left(\vec{S}_N \cdot \frac{\vec{q}}{m_N} \right)$$

$$\mathcal{O}_7^N = \mathbb{1}_X (\vec{S}_N \cdot \vec{v}_\perp)$$

$$\mathcal{O}_8^N = (\vec{S}_X \cdot \vec{v}_\perp) \mathbb{1}_N$$

$$\mathcal{O}_9^N = \vec{S}_X \cdot \left(\frac{i\vec{q}}{m_N} \times \vec{S}_N \right)$$

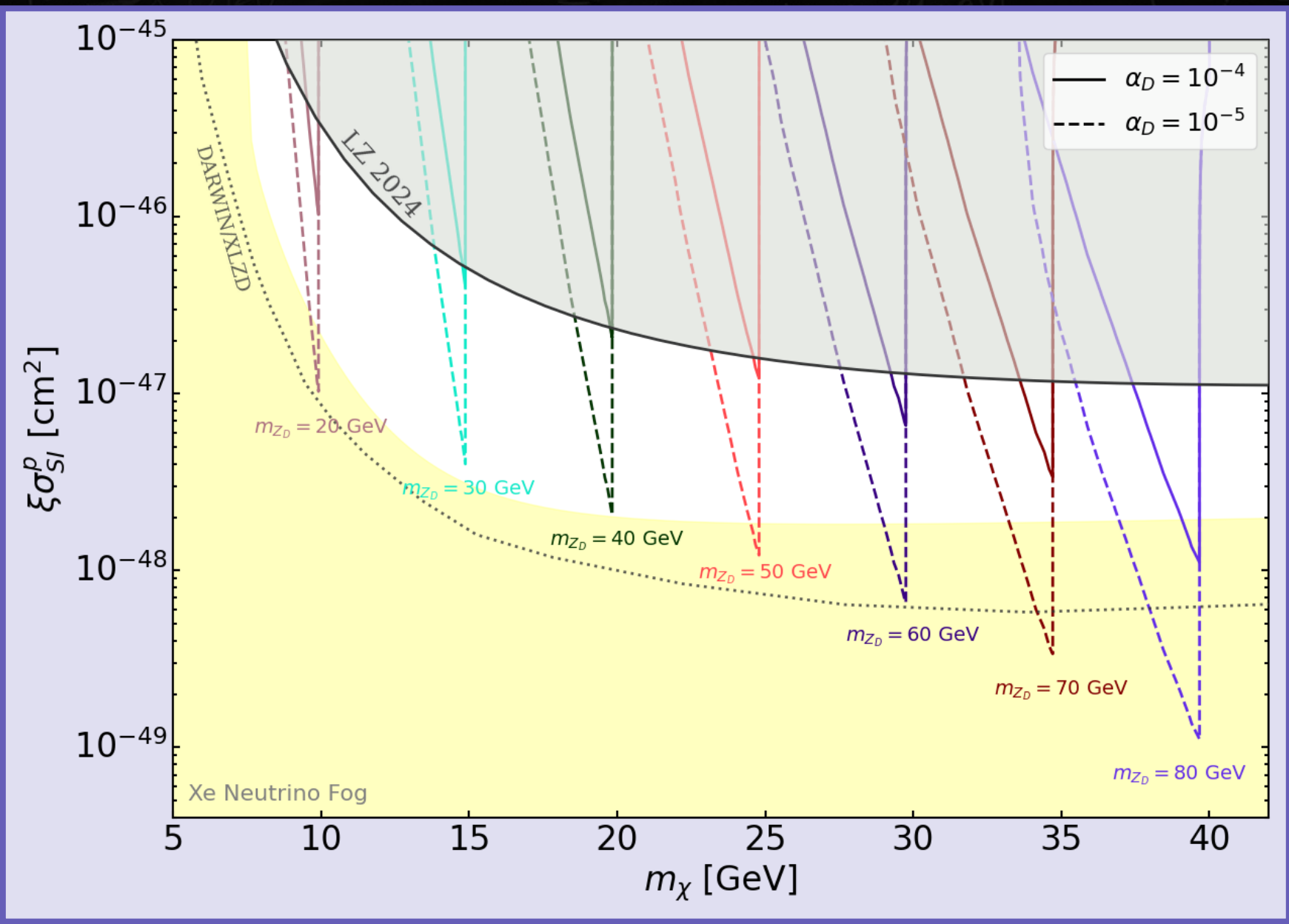
$$\mathcal{O}_{10}^N = -\mathbb{1}_X \left(\vec{S}_N \cdot \frac{i\vec{q}}{m_N} \right)$$

$$\mathcal{O}_{11}^N = - \left(\vec{S}_X \cdot \frac{i\vec{q}}{m_N} \right) \mathbb{1}_N$$

$$\mathcal{O}_{12}^N = \vec{S}_X \cdot (\vec{S}_N \times \vec{v}_\perp)$$

$$\mathcal{O}_{13}^N = -(\vec{S}_X \cdot \vec{v}_\perp) \left(\vec{S}_N \cdot \frac{i\vec{q}}{m_N} \right)$$

$$\mathcal{O}_{14}^N = - \left(\vec{S}_X \cdot \frac{i\vec{q}}{m_N} \right) (\vec{S}_N \cdot \vec{v}_\perp)$$



LZ collaboration (2025)
 DARWIN collaboration (2016)
 XLZD collaboration (2024)
 O'Hare (2021)

GAMMA RAYS STATISTICAL ANALYSIS

Fermi-LAT legacy analysis provides single-source, binned likelihood profiles $\mathcal{L}_i\left(\frac{d\phi}{dE}, E\right)$ as a function of the differential gamma ray flux $\frac{d\phi}{dE}$ and energy E for different sets of dSPhs source catalogues.

We can obtain the full model likelihood computing the theoretical $\frac{d\phi}{dE}$ and multiplying all the single-source likelihoods for the observed dSPhs.

For each source, the uncertainty on the observed J-factor is taken as a nuisance parameter:

$$\mathcal{L}_i(d\phi/dE, E, J_{obs}) = \frac{\mathcal{L}_i(d\phi/dE, E)}{\ln(10)\sqrt{2\pi}\sigma_J J_{obs}} \exp\left[-\left(\frac{\log_{10}(J) - \log_{10}(J_{obs})}{\sqrt{2}\sigma_J}\right)^2\right]$$

GAMMA RAYS STATISTICAL ANALYSIS

From the model likelihoods, we build a test statistic according to the profile log-likelihood ratio:

$$\log \lambda(\theta) = \log \frac{\mathcal{L}(\theta)}{\mathcal{L}(\theta_0)}$$

where θ denotes the model parameters and θ_0 the model parameters that maximize the likelihood.

Under random fluctuations in data, the test statistic $-2 \log \lambda(\theta)$ is asymptotically distributed as a χ^2 function with the number of degrees d equal to the number of tested parameters θ . Hence, for a fixed DM mass we leave the kinetic mixing freely floating.

We thus can reject the model at the $1 - p$ level if

$$1 - F_{\chi^2}(d = 1, -2 \log \lambda(\theta)) < p$$

with F_{χ^2} beint the cumulative χ^2 distribution with $d = 1$ d.o.f. We compute the one-sided 90% C.L. exclusion limit from $-2 \log \lambda(\theta) > 2.71$

CMB IONISATION CONSTRAINTS

$$P_{\text{ann}}(z) = \sum_i f_i(z) \frac{\langle \sigma v \rangle_i}{m_\chi}$$

We can compute approximate **mass-dependent efficiency factors** for all the primary annihilation channels of χ at $z \sim 600$ where energy injection becomes the most efficient

efficiency factors at $z = 600$

$$f_i(m_\chi) \approx \int_0^{m_\chi} \frac{E dE}{2m_\chi} \left[2f_{eff}^{e^+e^-}(E) \left(\frac{dN_{e^+}}{dE} \right)_i + f_{eff}^\gamma(E) \left(\frac{dN_\gamma}{dE} \right)_i \right]$$

secondary positron and photon spectra produced from EM showers and decays of the primary particles i

CMB IONISATION CONSTRAINTS

$$P_{ann}(z) = \sum_i f_i(z) \frac{\langle \sigma v \rangle_i}{m_\chi}$$

We can compute approximate **mass-dependent efficiency factors** for all the primary annihilation channels of χ at $z \sim 600$ where energy injection becomes the most efficient

efficiency factors at $z = 600$

$$f_i(m_\chi) \approx \int_0^{m_\chi} \frac{E dE}{2m_\chi} \left[2f_{eff}^{e^+e^-}(E) \left(\frac{dN_{e^+}}{dE} \right)_i + f_{eff}^\gamma(E) \left(\frac{dN_\gamma}{dE} \right)_i \right]$$

secondary positron and photon spectra produced from EM showers and decays of the primary particles i

Thus, we can define an **effective, mass-dependent annihilation parameter...**

$$P_{eff}(m_\chi) = \xi^2 \sum_i f_i(m_\chi) \frac{\langle \sigma v \rangle_i}{m_\chi}$$

... which is constrained by the Planck mission from CMB anisotropies measurement

$$P_{ann} < 3.5 \times 10^{-28} \text{ cm}^2 \text{ s}^{-1} \text{ GeV}^{-1}$$

EW PRECISION OBSERVABLES

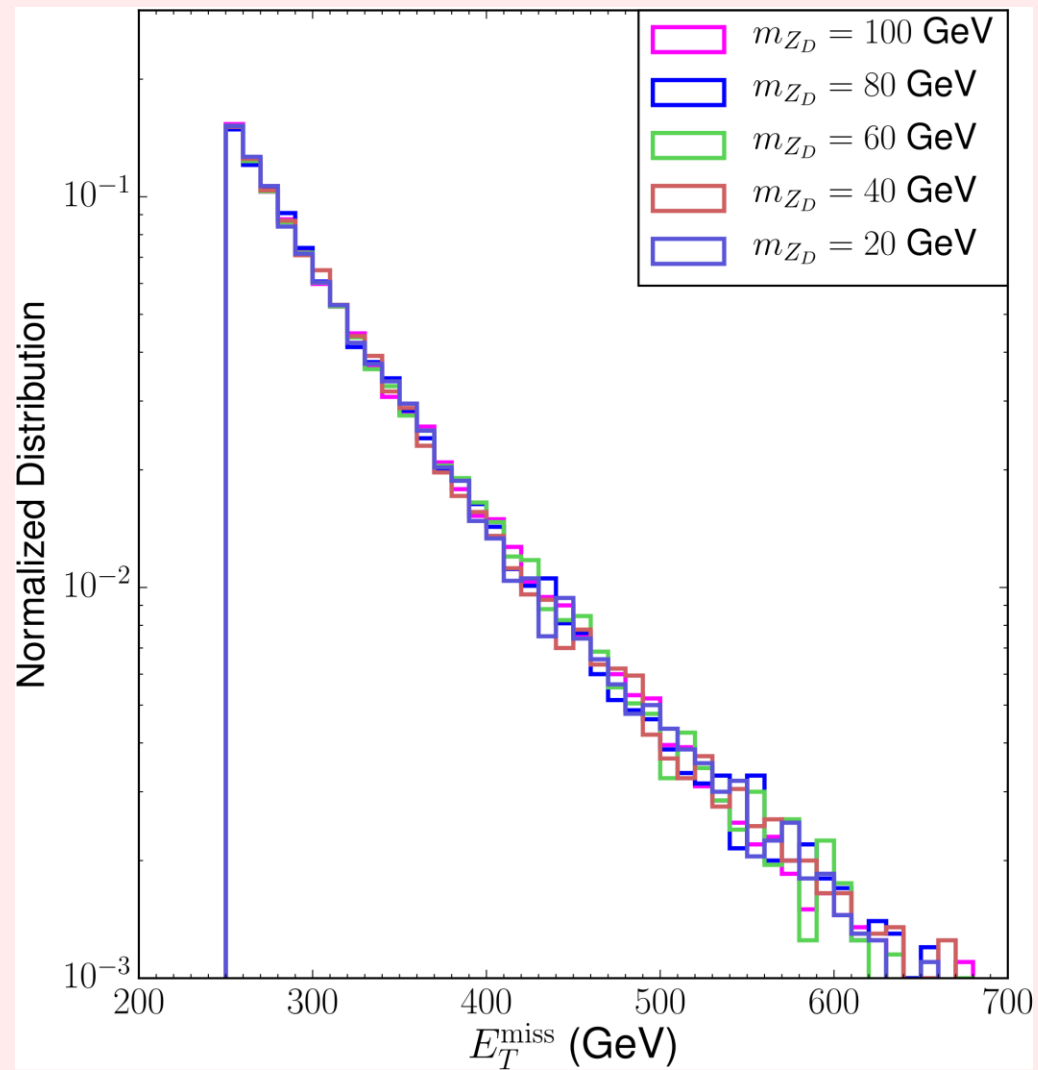
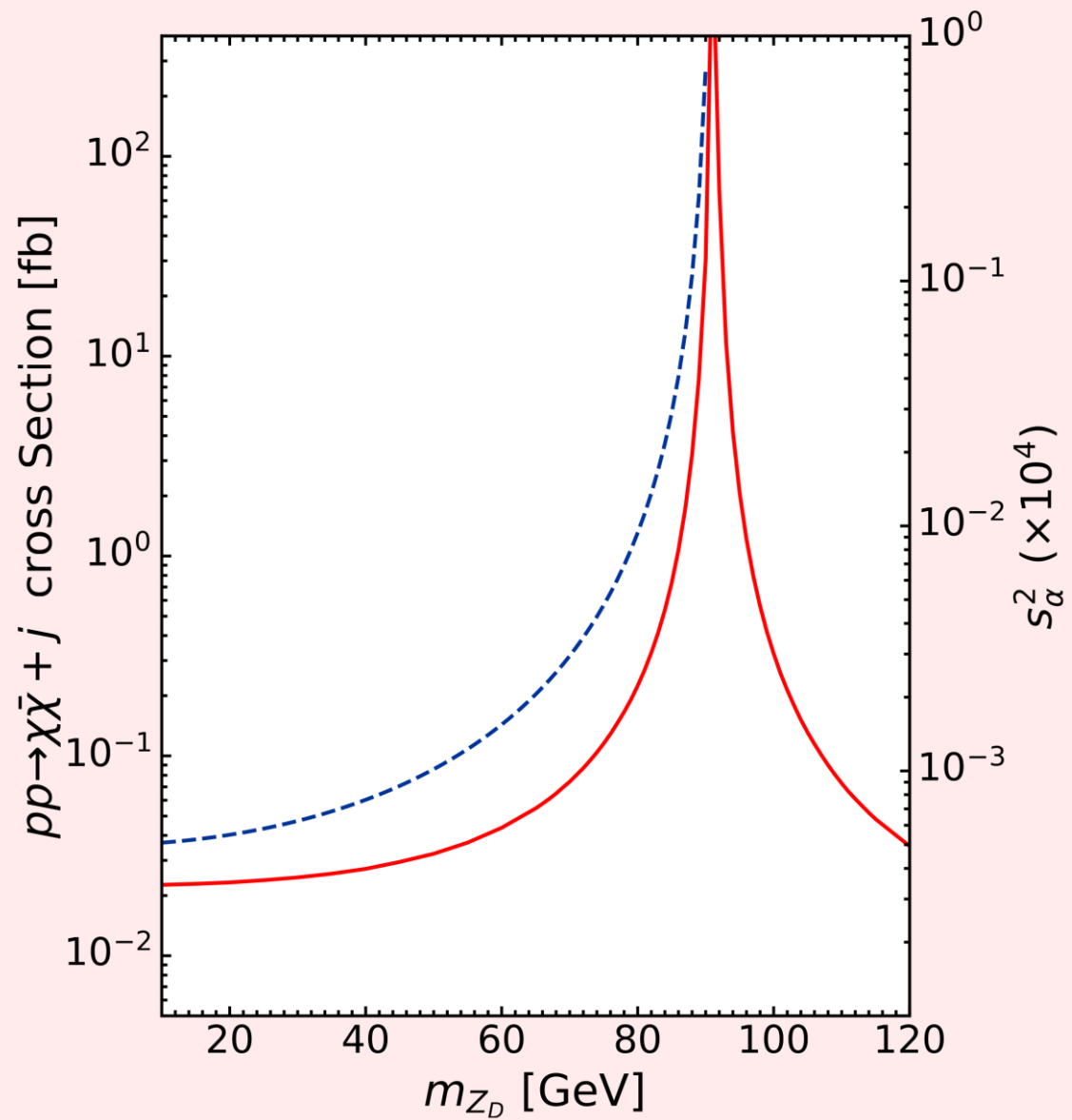
to derive the bounds from EWPO. We perform a χ^2 fit to $\mathcal{O}_1 = S(\epsilon, m_{Z_D})$ and $\mathcal{O}_2 = T(\epsilon, m_{Z_D})$, given by

$$\Delta\chi^2(\epsilon, m_{Z_D}) = \sum_{i,j} \left(\mathcal{O}_i(\epsilon, m_{Z_D}) - \mathcal{O}_i^0 \right) (\sigma^2)_{ij}^{-1} \left(\mathcal{O}_j(\epsilon, m_{Z_D}) - \mathcal{O}_j^0 \right), \quad (3.19)$$

with \mathcal{O}_i^0 denoting the central values in Eq. (3.18) and $(\sigma^2)_{ij} \equiv \sigma_i \rho_{ij} \sigma_j$, being σ_i the respective standard deviations from Eq. (3.18). The covariance matrix, ρ_{ij} , in the $S - T$ plane is given by [140]

$$\rho_{ij} = \begin{pmatrix} 1 & 0.92 \\ 0.92 & 1 \end{pmatrix}. \quad (3.20)$$

Our resulting 95% C.L. EWPO limits on ϵ as a function of m_{Z_D} (given by $\Delta\chi^2(\epsilon, m_{Z_D}) = 4$) agree well with those obtained in Ref. [58], and are shown in the left panel of Fig. 9 as a solid black-line. They yield the strongest current limits for a fully invisible dark photon (with $\text{BR}(Z_D \rightarrow \chi\bar{\chi}) = 1$) above the reach of B -meson factories like BaBar.



COLLIDER